

changes in the training/inference strategy, and reshaping of activation functions (AFs). However, most of them require additional computing resources, making its applicability to embedded systems difficult. Particularly interesting is the work in [5], where the authors observe that the least significant bits of the mantissa of the parameter values are weakly linked to accuracy. Accordingly, the authors present MATE, an error correction tool with no memory overhead based on the substitution of those bits by error correction codes for the weights. A different methodology is presented in [6], where the maximum values of the AFs are evaluated and then replaced with either lower or upper-bound values to reduce the propagation of errors through layers.

In this work we study the suitability of using bounded AFs as a means to improve the robustness of image segmentation DNNs and how this choice can impact the performance and implementability of these models. With this aim, we analyze the process of deploying an encoder-decoder DNN on an FPGA for a real-world task: the semantic segmentation of hyperspectral images in the context of autonomous driving.

Section II describes how the DNN under study has been developed in terms of selection of the AFs, training, pruning, and quantization for deployment on edge devices. In Section III, we analyze the effects of applied compression techniques on model robustness according to the choice of the AFs by means of an statistically significant FI campaign. In Section IV, we give details about the deployment of the models on an FPGA and report comparative performance figures. Finally, the concluding remarks are presented in Section V.

II. MODELS' DEVELOPMENT

The reference segmentation model in this study is a U-Net, an encoder-decoder fully convolutional network for image segmentation tasks. This DNN has been adapted to use hyperspectral images (HSI) from HSI-Drive v2.0 [7], a dataset intended for developing ADS systems using HSI. The most recent version, described in [8], is based on a 5-level encoder-decoder architecture containing two sequences of 3×3 *conv2D* layers (initially with 32 filters) followed by Batch Normalization and Rectified Linear Unit (ReLU) AFs at each level. Additionally, it includes one 2×2 Max-pooling 2D layer per encoder level and one 2×2 *conv2D_{tr}* layer per decoder level. The resulting model features 31.14 million parameters and requires 34.60 GFLOPS per inference to execute.

Since the lack of bounds in most widely used AFs for DNN implementation (e.g. ReLU) facilitates the propagation of soft errors, in this article we also explore the use of squashing AFs, such as Sigmoid and Hard Sigmoid, being the latter a more basic, computationally efficient version of the former [9]. The objective is to analyze their potential benefits on model robustness, while also assessing their impact on performance and implementability. The DNNs have been designed with *TensorFlow2* and trained on a Dell Precision 7920 Workstation equipped with an NVIDIA RTX 3090 GPU.

TABLE I: IoU of 32-bit floating-point DNNs on the test set.

Class \ AF	ReLU	Sigmoid	Hard Sigmoid
Road	97.84	96.94	96.32
Marks	87.99	82.88	83.43
Vegetation	94.23	92.53	92.39
Sky	92.83	89.47	85.17
Others	78.12	76.38	69.07
Global	94.71	93.32	92.02
Weighted	88.54	84.75	82.69

A. Reference model's performance

First, the three AFs are evaluated based on their performance in training and testing using the reference noncompressed model. The Sigmoid-based and Hard Sigmoid-based models required 1000 epochs, while the ReLU-based DNN, which allows for faster convergence, was trained for only 200 epochs. Table I shows the best Intersection Over Union (IoU) results of the 32-bit floating-point DNNs on the test set according to the used AF.

The best metrics are obtained for the ReLU model, although in all three cases, the Global IoU (GIoU) is above 92%. The Weighted IoU (WIoU), which is calculated by weighting each class by the inverse of its frequency in the dataset, is above 82%. These results are considered satisfactory given the highly unbalanced nature of the dataset [7].

B. Model pruning

For this model to be implemented on an edge device, it is necessary to apply certain compression techniques such as pruning and quantization. Channel pruning aims to reduce both the number of parameters and the number of FLOPS by removing channels that have minimal impact on the output. This is achieved through a model sensitivity analysis which consists of gradually pruning (in increments of 0.1 in our case) each of the parameters, while the rest of the model remains frozen, to estimate which layers are the least essential ones. After choosing an overall pruning ratio in terms of FLOPS, each of the layers is pruned accordingly, and then the DNN is fine-tuned for a certain number of epochs (60 for ReLU and 200 for the other two AFs) to recover any lost accuracy.

This process is repeated twice for each model in what is known as iterative pruning, thus requiring the whole process to be repeated on the pruned model after the first iteration. To consider pruning as valid, a maximum degradation of 1.5 points in both GIoU and WIoU has been accepted, ensuring both remain above 90% and 80%, respectively.

The overall pruning ratios have been: 0.75 (0.5 and 0.5) for the ReLU-based model, 0.52 (0.4 and 0.2) for the Sigmoid-based model, and 0.7 (0.5 and 0.4) for the Hard Sigmoid-based model. Fig. 1 illustrates the pruning ratio applied to each layer, where it can be noted that, even though the overall pruning ratio of the ReLU-based DNN and the Hard Sigmoid-based model are very similar, the individual pruning ratio greatly varies from layer to layer, especially in the initial layers of the encoder and the final layers of the decoder. It can also be seen that, from layer *cnv_6* to layer *cnv_15*, which are the

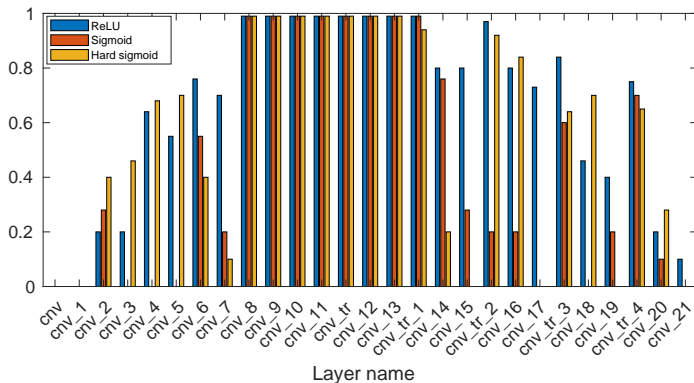


Fig. 1: Overall pruning ratio in each of the layers in the models with ReLU (0.5 and 0.5), Sigmoid (0.4 and 0.2) or Hard Sigmoid (0.5 and 0.4) AFs.

ones placed around the base, the Sigmoid-based DNN is more pruned than the Hard Sigmoid-based DNN.

As the layers next to the base of the architecture are the ones that contain most of the parameters, even though the overall pruning ratio in terms of FLOPS is smaller for the Sigmoid-based DNN, it results in a model containing fewer parameters than the Hard Sigmoid-based DNN. Table II shows the complexity and size of the models, which have been significantly reduced after the pruning process.

C. Quantization

Quantization is another compression technique aimed at reducing the size of the parameters to store and accelerating model inference when deployed on customized hardware. In this article, we apply a homogeneous post-training quantization scheme where all parameters and activations are converted to 8-bit integers. For further details on the quantization process, the reader is referred to [10]. It is worth noting that after quantization, the Sigmoid-based model has experienced a noticeable degradation. To recover the lost accuracy, a process called fast finetuning has been carried out.

III. ANALYSIS OF ROBUSTNESS AGAINST SBUS

To test the models' robustness against SBUs, an extensive FI campaign was conducted on the aforementioned models, which involved injecting single bit-flips into the parameters of the DNNs. Perturbations were inserted using our modified version of the original *TensorFI2* framework [4], and the code is shared at <https://github.com/jonGuti13/TensorFI2>. To ensure the statistical significance, which is very important as stated in [11], of the performed FI campaign 1550 different

TABLE II: DNN complexity and size reduction after applying channel-pruning and quantization.

Metric \ AF	Original	ReLU	Sigmoid	Hard Sigmoid
Params (M)	31.13	0.32	1.38	1.47
OPS (G)	34.59	8.41	16.46	10.35
Memory (MB)	249.04	2.49	11.04	11.76

soft errors per parameter set (a 2.5% error margin, a 95% confidence level, and a 50% failure probability to maximize sample size [12]) have been injected. To evaluate the impact of the FI campaign, it is first necessary to define what an inference error is. A bit-flip is considered to have caused an error if the predicted class at any pixel in the test images changes with regard to the prediction made by the unperturbed original model, i.e., critical errors. The error rate is therefore presented as a percentage between 0 and 100, with 100 representing the situation where a bit-flip has changed the predicted class of every single pixel.

A. Original noncompressed models

Fig. 2 displays the error rate for each parameter set and flipped bit for the ReLU-based 32-bit floating-point DNN (for an in-depth analysis of this model the reader is referred to [8]). Only sign and exponent bits are shown because perturbations in mantissa bits generate a negligible amount of errors. Even though Fig. 2 varies for each of the nonquantized DNNs under study (nonpruned/pruned and ReLU/Sigmoid/HardSigmoid), they also share a common pattern.

Firstly, errors primarily occur as a consequence of the increment of the perturbed parameters' values. Secondly, the most sensitive bit is the MSB bit of the exponent as it is originally a '0' in most of the DNNs parameters (the ones in $0 \leq |x| < 2$ range). In fact, if the original parameter value is 1 or is in $1 < |x| < 2$ range, a bit-flip converts the parameter into a $\pm\infty$ or a *NaN*, respectively. Thirdly, the most sensitive parameter is the gamma set of Batch Normalization layers as it usually has a value near 1. Finally, leaving aside the MSB, the most sensitive zones are the initial layers of the encoder and the final layers of the decoder, which are both directly connected to the output as a consequence of the skip-connections typical of encoder-decoder architectures.

Fig. 3 displays a comparison of measured mean error rates of each parameter set for the three AFs. The error rates are

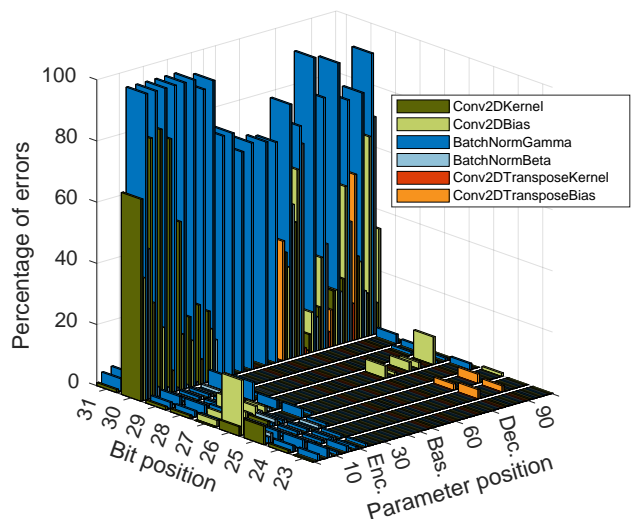


Fig. 2: Bit-flip error rate for the original ReLU-based DNN.

smaller for the DNNs with squashed AFs, especially in the kernel/bias parameters of the *Conv2D* layers, benefiting from the fact that faulty parameter values cannot grow indefinitely, and neither can the error. The Hard-Sigmoid-based model exhibits the highest level of robustness.

Another aspect that differs as a consequence of the AF used is the range of parameter values. As explained, a range considered to be potentially dangerous is $1 < |x| < 2$. In Fig. 4, the difference between the MSB bit-flip error rate and the ratio of parameter set values in $1 < |x| < 2$ is displayed. Minor negative peaks are a consequence of the statistical FI campaign where not all the parameters per set are perturbed.

Fig. 4 shows how the MSB bit-flip errors in the central area of the U-Net, which is composed of the last layers of the encoder, the base, and the first layers of the decoder, mainly occur because of the MSB bit-flip of the parameters which are in the $1 < |x| < 2$ interval. At the same time, we can also see the benefits of using bounded AFs as the MSB bit-flip error rate is smaller than in ReLU based DNN.

B. Pruned models

In this subsection it is analyzed to what extent the vulnerability of the DNNs against SBUs changes as a consequence of the pruning process described in Section II-B. From the comparison between Fig. 3 and Fig. 5 it can be concluded that the error rate has augmented after the DNNs have been pruned. However, the three models have not experienced an equal loss of robustness. The more over-parameterized a model is, the greater the likelihood that a bit-flip will occur on a less critical parameter, thus not impacting the predicted classes. Indeed, the two most pruned models (ReLU and Hard Sigmoid) have shown the most degradation, while the Sigmoid-based DNN now exhibits the highest robustness, surpassing the Hard-Sigmoid in terms of mean bit-flip error rate (as indicated by the black bar in Fig. 5). Nevertheless, albeit marginally, the Hard-Sigmoid demonstrates a lower standard deviation, suggesting less variability in the bit-flip error rate across different positions.

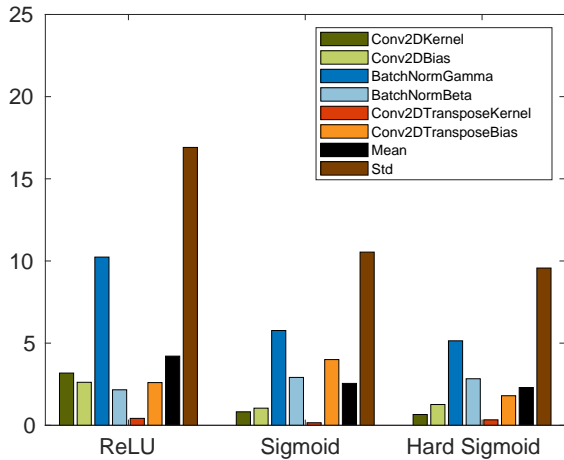


Fig. 3: Mean bit-flip error rate in the original model.

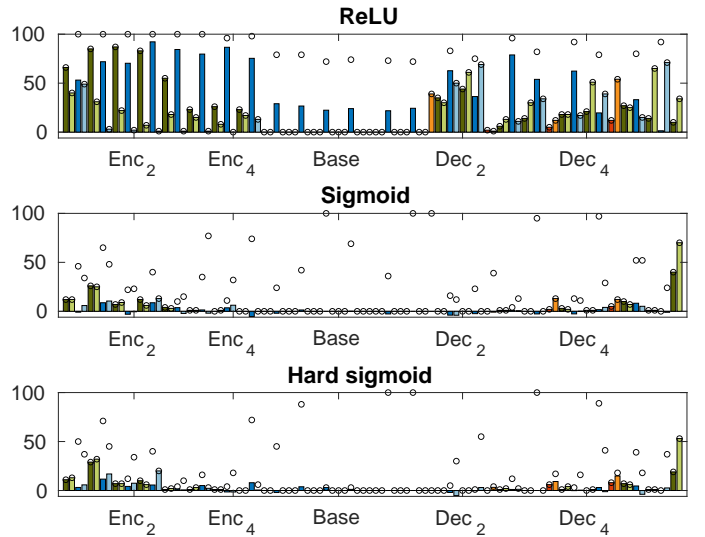


Fig. 4: Difference between MSB bit-flip error rate and ratio of parameter set values in $1 < |x| < 2$. Unfilled dots indicate MSB bit-flip error rate. Original model.

From this analysis, it may seem that pruning is only recommended for reducing the complexity of DNNs and accelerating their inference, and that it has detrimental effects on their robustness. However, in most implementations, the probability of a SEU occurring in smaller models is also lower due to decreased device occupation, so to accurately assess the influence of pruning on vulnerability to SEUs, factors such as circuit design and chosen target device must be considered.

Pruning also increases the proportion of values in the range $1 < |x| < 2$ by removing channels with parameters that are usually close to 0 and considered irrelevant.

As shown in Fig. 6, the central region of the ReLU-based DNN has the fewest errors, with most errors resulting from bit-flips in parameters within the range $1 < |x| < 2$. This pattern also holds for bounded AFs, where almost all errors in the central region are due to this kind of bit-flips.

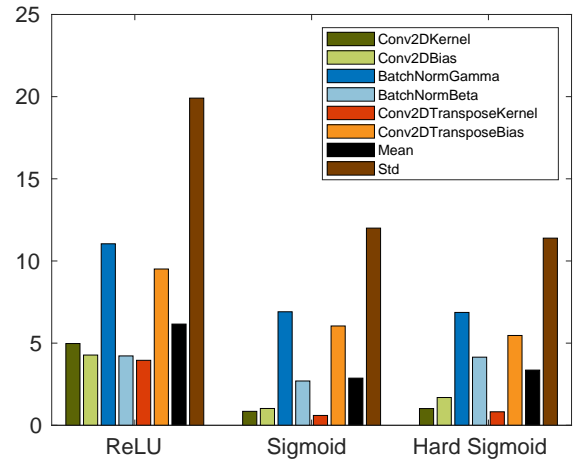


Fig. 5: Mean bit-flip error rate in the pruned model.

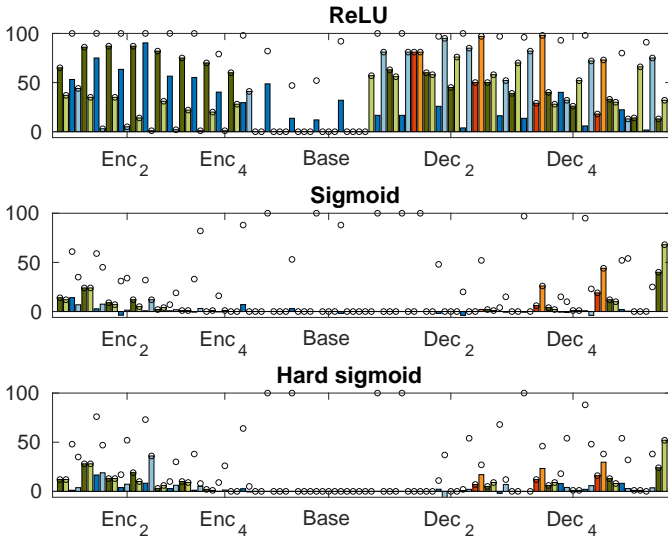


Fig. 6: Difference between MSB bit-flip error rate and ratio of parameter set values in $1 < |x| < 2$. Unfilled dots indicate MSB bit-flip error rate. Pruned model.

C. Pruned quantized models

Finally, the combined effects of applying pruning and full integer quantization are assessed. Since this is a general analysis based on simulations, we used *TensorFlow Lite*'s quantization scheme [13] to evaluate robustness against SBUs, while the AMD-Xilinx's Vitis AI tool quantization was applied for final implementation (see Section II-C). The main difference is that *TensorFlow Lite* uses a 32-bit integer representation instead of a 8-bit integer representation for biases (however, we verified that the variation in GIoU is below ± 0.08 between both schemes). According to [13], the quantized version \hat{r} of a real number r is approximated by (1), where S is a positive real scale factor, q is an 8/32-bit integer value, and Z is the zero-point, an integer value which is 0 for symmetric quantization.

$$\hat{r} \approx r = S(q - Z) \quad (1)$$

Thus, the value q_y resulting from $Y = Wx + b$ is:

$$q_y = \frac{S_w S_x}{S_y} (q_w q_x - Z_x q_w + q_b) \quad (2)$$

Due to the per-tensor and mainly symmetric quantization scheme, the number of q_i values to store is significantly greater than that of Z_i and S_i values, so bit-flips were only injected on q_w and q_b . The results for the pruned and quantized ReLU-based model are shown in Fig. 7. Although the quantized model may initially seem less robust than its nonquantized counterpart, in this case only the biases are sensitive parameters. Since biases make up an small part of the model, the overall proportion of sensitive parameters is much smaller than in the nonquantized model. Regarding the comparison among AFs, bounded ones consistently offer greater robustness to the model as depicted in Fig. 8.

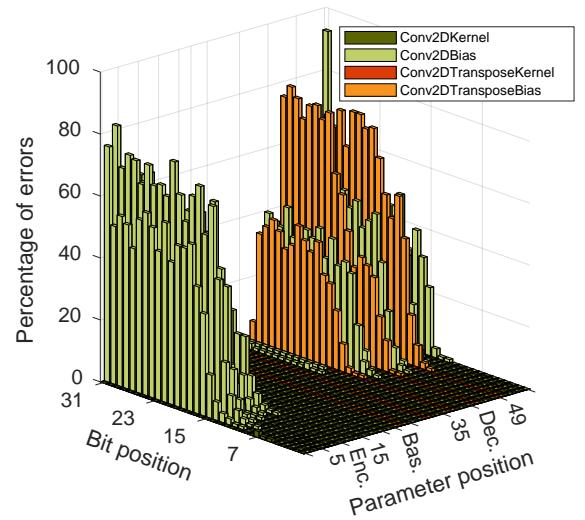


Fig. 7: Bit-flip error rate for the pruned quantized ReLU-based DNN (weights are 8-bit long and biases are 32-bit long).

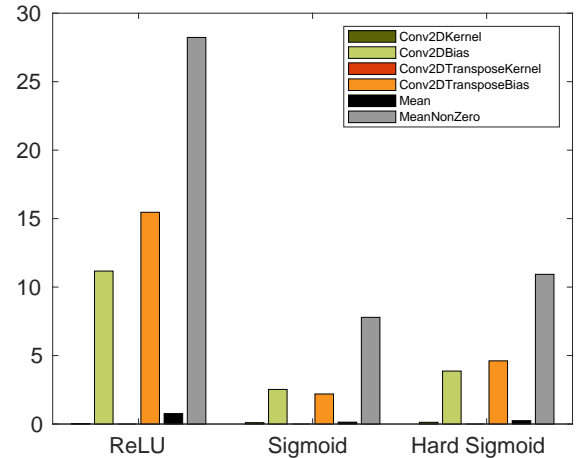


Fig. 8: Mean bit-flip error rate in the pruned quantized model.

IV. DEPLOYMENT AND PERFORMANCE CHARACTERIZATION

The DNNs were implemented on an AMD-Xilinx K26 SoM, which features an XCK26-SK-KV260-G Zynq UltraScale+ MPSoC containing a 64-bit Quad-Core ARM A-53 processor along with a 16nm FinFET Programmable Logic FPGA. The DNNs have been deployed using AMD-Xilinx's Vitis AI 3.5 environment on a single-core B4096 Deep Processing Unit (DPU). To characterize the performance of the models, the IoU on the test images, the throughput and the power consumption during DPU inference were measured on the KV260 SoM running Petalinux operating system (see Table III).

Throughput measurements were conducted by averaging the inference execution of 100 iterations on the test images. The fact that the ReLU-based model was the most compressed after pruning, combined with the simplicity of calculating the AF, results in the highest throughput among the three, closely followed by the Hard Sigmoid-based model. Since the Sigmoid

TABLE III: IoU of the pruned 8-bit integer DNNs on the test set.

Class \ AF	ReLU	Sigmoid	Hard Sigmoid
Road	97.72	96.01	96.74
Marks	88.15	82.73	81.07
Vegetation	93.85	88.94	90.76
Sky	92.45	82.82	82.05
Others	77.38	65.73	69.95
Global	94.47	90.67	91.80
Weighted	88.37	80.96	80.72

function is not piecewise linear, its direct implementation on a DPU is unsupported and must be computed on a CPU core, thus dramatically augmenting the inference latency.

Power consumption in the SoM was measured using the *tegrastats* application thanks to the INA260 current sensor integrated in the KV260. The Sigmoid-based DNN deployment consumes the least power since AFs are computed on the CPU, but its slow execution makes it the most energy-intensive, which is estimated by multiplying the inverse of the throughput by the mean power consumption. On the contrary, the ReLU-based implementation is the most energy efficient.

V. CONCLUSIONS

This article explores the use of bounded AFs in image segmentation DNNs to assess the robustness of these models against soft errors when deployed on embedded processing platforms for safety-critical applications. As a general conclusion, we found that it is a trade-off between the resilience enhancements that bounded squashing AFs provide and the need for more aggressive model compression to improve computational performance and reduce memory footprint.

Regarding pruneability, ReLU-based and Hard Sigmoid-based models prove to have the larger pruneability factors, achieving a reduction in the number of parameters by over 95% and a reduction in the number of GFLOPS by over 70% in both cases. When it comes to robustness against single bit-flips, bounded AFs show the best resilience as the propagation of generated perturbations throughout the model layers is notably reduced. In 32-bit floating-point models, the most critical situation occurs when a bit-flip affects the MSB of the exponent for values in the range $1 < |x| < 2$, resulting in a conversion to *NaN*. This primarily affects the Gamma parameters in Batch Normalization layers. The over-parameterized nature of the original DNNs imply that as a model is pruned deeper, it seems to lose robustness. However, the relative difference between ReLU-based and

TABLE IV: Characterization of the optimized models with different AFs on the KV260 SoM.

Metric \ AF	ReLU	Sigmoid	Hard Sigmoid
Throughput (FPS)	22.68	0.59*	19.83
Power (W)	6.62	5.74*	6.90
Energy (J)	0.29	9.73	0.35

*Activation runs on CPU.

Hard Sigmoid-based models, both with similar pruning ratios, remains constant. Nevertheless, the advisability of applying pruning techniques in relation to its influence over robustness must be contrasted with the particular design of the processor for deployment, since smaller models generally require fewer logic resources, decreasing the likelihood of an SBU occurring in a sensitive parameter. For pruned and quantized integer models, the inherent binary representation prevents the occurrence of *NaNs* or infinities, significantly reducing the error rate, while the relative robustness between different AFs show an identical pattern.

In terms of IoU, for DNNs implemented on an AMD-Xilinx KV260 SoM, the ReLU-based model achieved the best results. This, combined with the computational complexity and high latencies of computing Sigmoid AF, makes the ReLU-based DNN the most efficient in terms of throughput and power consumption. However, using Hard-Sigmoids as nodal AF deserves to be considered as a suitable design option for a good trade-off between robustness and performance.

REFERENCES

- [1] M. H. Ahmadiilivani, M. Taheri, J. Raik, M. Daneshtalab, and M. Jenihhin, "A systematic literature review on hardware reliability assessment methods for deep neural networks," *ACM Comput. Surv.*, dec 2023. Just Accepted.
- [2] S. Hong, P. Frigo, Y. Kaya, C. Giuffrida, and T. Dumitras, "Terminal brain damage: Exposing the graceless degradation in deep neural networks under hardware fault attacks," in *28th USENIX Security Symposium (USENIX Security 19)*, pp. 497–514, 2019.
- [3] N. Narayanan, *Fault injection in Machine Learning applications*. PhD thesis, University of British Columbia, 2021.
- [4] N. Narayanan, Z. Chen, B. Fang, G. Li, K. Pattabiraman, and N. DeBardeleben, "Fault injection for tensorflow applications," *IEEE Transactions on Dependable and Secure Computing*, vol. 20, no. 4, pp. 2677–2695, 2023.
- [5] M. Jang and J. Hong, "Mate: Memory-and retraining-free error correction for convolutional neural network weights," *Journal of Information & Communication Convergence Engineering*, vol. 19, no. 1, 2021.
- [6] M. Taheri, N. Cherezova, M. S. Ansari, M. Jenihhin, A. Mahani, M. Daneshtalab, and J. Raik, "Exploration of activation fault reliability in quantized systolic array-based dnn accelerators," 2024.
- [7] J. Gutiérrez-Zaballa, K. Basterretxea, J. Echanobe, M. V. Martínez, and U. Martínez-Corral, "Hsi-drive v2. 0: More data for new challenges in scene understanding for autonomous driving," in *2023 IEEE Symposium Series on Computational Intelligence (SSCI)*, pp. 207–214, IEEE, 2023.
- [8] J. Gutiérrez-Zaballa, K. Basterretxea, and J. Echanobe, "Evaluating single event upsets in deep neural networks for semantic segmentation: An embedded system perspective," *Journal of Systems Architecture*, vol. 154, p. 103242, 2024.
- [9] A. Apicella, F. Donnarumma, F. Isgrò, and R. Prevete, "A survey on modern trainable activation functions," *Neural Networks*, vol. 138, pp. 14–32, 2021.
- [10] J. Gutiérrez-Zaballa, K. Basterretxea, J. Echanobe, Ó. Mata-Carballeira, and M. V. Martínez, "Rapid deployment of domain-specific hyperspectral image processors with application to autonomous driving*," in *2023 30th IEEE International Conference on Electronics, Circuits and Systems (ICECS)*, pp. 1–6, 2023.
- [11] A. Ruospo, G. Gavarini, C. De Sio, J. Guerrero, L. Sterpone, M. S. Reorda, E. Sánchez, R. Mariani, J. Aribido, and J. Athavale, "Assessing convolutional neural networks reliability through statistical fault injections," in *2023 Design, Automation & Test in Europe Conference & Exhibition (DATE)*, pp. 1–6, IEEE, 2023.
- [12] R. Leveugle, A. Calvez, P. Maistri, and P. Vanhauwaert, "Statistical fault injection: Quantified error and confidence," in *2009 Design, Automation & Test in Europe Conference & Exhibition*, pp. 502–506, 2009.
- [13] B. Jacob, S. Kligys, B. Chen, M. Zhu, M. Tang, A. Howard, H. Adam, and D. Kalenichenko, "Quantization and training of neural networks for efficient integer-arithmetic-only inference," 2017.